Proceedings of the 10th World Congress on Mechanical, Chemical, and Material Engineering (MCM'24)
Barcelona, Spain - August 22-24, 2024
Paper No. ICCPE 119
DOI: 10.11159/iccpe24.119

Water Adsorption Capacity of UiO-66 Metal Organic Framework (MOF) Nanoparticles for Applications in Water Harvesting

Selis Onel[1,2], Anil Hatiboglu[2], Saziye Dere[1,3]
[1]Hacettepe University, Department of Chemical Engineering
Beytepe, Ankara, Turkiye
selis@hacettepe.edu.tr
[2]Hacettepe University, Institute of Science
Beytepe, Ankara, Turkiye
anilhatiboglu@hacettepe.edu.tr
[3]Malatya Science High School
Yesilyurt, Malatya, Turkiye

Abstract – Metal organic framework (MOF) nanoparticles, characterized by their substantial surface area, tunable porosity, and exceptional adsorption capacity, emerge as promising candidates for water harvesting via efficient water vapor capture in arid regions. This investigation presents an experimental evaluation of zirconium-based UiO-66 MOF nanoparticles exposed to both liquid water and controlled humidity conditions. FTIR spectroscopic analysis revealed distinct spectral signatures associated with O-H bonds for dry and wetted UiO-66 particles. Dry UiO-66 particles kept at five different relative humidity conditions demonstrated different performances with increased water adsorption capacity at elevated humidity values, consistent with the porous structure of MOF particles and previous literature. Comparative analysis of UiO-66 adsorption behaviour in both liquid and vapor phases provides valuable insights into the feasibility of utilizing these materials for water harvesting applications.

***Keywords*:** Metal organic framework (MOF), UiO-66, Water adsorption, Water harvesting

1. Introduction

Due to advancements in technological developments, zeolites, metal oxides, carbon nanotubes, graphene oxides, and metal organic framework (MOF) structures are being increasingly utilized as adsorbents and inorganic filler materials in polymer composites. Among these structures, particles with MOF structures stand out due to their remarkable properties, including high surface area-to-volume ratio providing an immense platform for molecular interactions, tunable porosity, exceptional adsorption capacity, and compatibility with polymer chains [1]. Enhanced adsorption properties allow for efficient capture and storage of water vapor posing a potential solution for water harvesting in arid regions or for emergency water supplies.

MOF crystals are constructed by the assembly of metal ions linked together by organic ligands, which act as molecular bridges [2]. This combination of various metal and organic linkages gives rise to porous materials that can exist in either crystalline or amorphous forms. At the heart of MOF structures lie metal ions, such as Zr, Cr, Ti, and Al, which serve as the connecting nodes, linked together by organic bridging ligands, including polycarboxylates, polypyridines, and polyterephthalic acids. These intricate arrangements give rise to three-dimensional frameworks, offering a unique combination of properties. Their ability to maintain stability even at temperatures exceeding 200 °C, coupled with their low density, high crystallinity, and exceptional surface areas, makes them truly exceptional materials. These hybrid materials, seamlessly blending the characteristics of both organic and inorganic porous materials, have opened up a plethora of opportunities in diverse fields, ranging from purification and drug delivery to energy storage and catalysis. One of the earliest MOF crystals synthesized, MIL-47 based on vanadium [3], has found applications in adsorption, catalysis, and lithium-ion batteries. MIL-125, a titanium-based MOF, boasts a high surface area, exceptional thermal stability, and environmental benignity, making it a versatile material for separation and catalysis applications [4]. UiO-66 crystals, constructed from zirconium, are prized for their thermal resistance and wide-ranging applications, including gas storage [5-7].

The growing demand for clean drinking water and the depletion of freshwater resources due to climate change have prompted researchers to explore innovative water harvesting technologies [8]. UiO-66 has emerged as a promising material for capturing water vapor and exhibits excellent stability in humid environments making it a reliable material for long-term use [9]. UiO-66 particles can be integrated into practical devices, such as humidity sensors [10], water harvesting systems [11], humidity regulation systems for greenhouses and vertical farms, or targeted water delivery systems for localized control in a field. Compared to conventional adsorbents like zeolites and silica materials, UiO-66 demonstrates a lower desorption temperature, indicating that the captured water can be released with less energy input. This energy efficiency is crucial for sustainable water harvesting processes.

This study aims to investigate the water adsorption capacity of zirconium (Zr)-based UiO-66 structures under different humidity environments. The MOF structure consists of cationic $Zr_6O_4(OH)_4$ nodes and 1,4-benzenedicarboxylate (BDC) linkers. Its thermal and chemical stability is attributed to the strong bonds between carboxylate oxygens and Zr atoms. UiO-66 exhibits high chemical resistance to water and organic solvents across a wide pH range. The strong Zr-O bonds within its structure enhance its structural stability. The cubic unit cell of the UiO-66 structure comprises eight tetrahedral cages surrounding one octahedral cage and contains eight pores. The results demonstrate that UiO-66 effectively captures water from humid air, even at low humidity levels serving it as a promising material for water harvesting applications in regions facing water scarcity.

2. Materials and Methods

Commercially available analytical grade chemicals were procured from Sigma-Aldrich (St. Louis MO, USA) for all experimental procedures. The precursor solution was prepared using n,n-dimethylformamide (DMF, 99%) as the solvent, terephthalic acid (H_2BDC) as the organic ligand, and zirconium (IV) chloride ($ZrCl_4$) as the metal salt. Hydrochloric acid (HCl, 37%) was employed as modulator. Acetone was utilized for washing the particles. The preparation of the precursor solution involved precise measurement of all chemicals using a balance for solids and micropipettes for liquids. Metal salt was dissolved in 5 mL of DMF, and the organic ligand was dissolved in another 5 mL of DMF, both aided by sonication for 20 minutes. The metal salt and organic ligand solutions were combined in a closed glass vial with the modulator and sonicated for an additional 10 minutes to ensure complete mixing.

2.1. Synthesis of nanoparticles

UiO-66 was synthesized from the precursor solution via a solvothermal route at 100 °C for 24 hours. This batch of UiO-66 is named as B1:1:80:1HCl:24h:100C based on the final mole ratio in the order of the metal salt (ZrCl4), organic ligand (H_2BDC), solvent (DMF), and modulator HCl, synthesis time h in hours, and temperature C in °C. At the elapse of the synthesis time, the glass vial was removed from the oven and allowed to cool down to ambient temperature. The resulting particles were subjected to washing at least three times with acetone. Following each wash, the particles were centrifuged at 5000 rpm for 5 minutes to facilitate separation from the cleaning solvent. The washed particles were dried at 80 °C to obtain the clean powder of porous UiO-66 MOF nanoparticles.

2.2. Liquid Water Adsorption

UiO-66 MOF samples were subjected to oven drying at 110 °C to eliminate residual solvents and possible moisture uptake. Dried UiO-66 samples were accurately weighed and transferred to small vials, i.e. sequentially numbered 5 ml Eppendorf tubes from 1 to 8. Varying amounts of ultrapure water just enough to completely wet the particles were added to each vial using micropipettes. The vials were resealed and allowed to equilibrate for a specified time. The vials were weighed again to determine the amount of water added on the UiO-66 samples in the vial calculated based on the weight difference. Vial 1 served as a control, containing solely dry UiO-66 nanoparticles without any liquid water. Vials 2-8 were prepared with varying amounts of UiO-66 exposed to different water loadings. For all samples, the amount of water added was more than the nanoparticles available by weight to ensure that the water in each vial exceeded the water uptake capacity of UiO-66 reported as 0.51 $g \cdot g^{-1}$ [12]. The amount of water added to vial 5 greatly exceeded the other vials, but it was retained for observational purposes without alteration.

Wet UiO-66 samples from each vial were characterized by their Fourier transform infrared (FTIR) (Thermo Scientific Nicolet 6700 FT-IR spectrome) spectra in the range between 3700 cm^{-1} and 2852 cm^{-1}, which covers the stretching vibration envelope of the O-H bond [13].

2.3. Water Vapor Adsorption

Dried and weighed UiO-66 samples were subjected to various relative humidity (RH) conditions of 27%, 42%, 50%, 60%, and 75% in an isolated precision balance. A saturated KOH aqueous solution was prepared to reach an RH of 27%, which was less than the RH in ambient conditions. NaCl aqueous solutions of varying concentrations were prepared to create higher humidity environments. Initial observations were made at 30 °C and 30% RH. Measurements were recorded at regular time intervals. Each measurement was continued until the sample weight reached a constant value. The relationship between RH and water adsorption capacity of UiO-66 particles was examined. All measurements were performed in duplicate. FTIR spectra were recorded for each sample to identify and characterize the interactions between the MOF nanoparticles and water molecules.

3. Results and Discussion

Water adsorption of different amounts of UiO-66 nanoparticles wetted in surpassing amounts of liquid water was investigated using FTIR analysis based on the analysis of O-H groups acting as active sites for interfacial water. A previous FTIR investigation of water adsorption on cellulose nanofiber films has shown three spectral regions 3700-2538 cm^{-1} (studied as 3700–3000 cm^{-1}, 3700-2852 cm^{-1}, and 2852–2538 cm^{-1}), 1740–1618 cm^{-1}, and 1190–1139 cm^{-1} related to water adsorption [12]. In this study, the main FTIR peaks associated with water adsorption are assigned between wavenumbers 3700-2852 cm^{-1} as O-H stretching vibration and at 1640 cm^{-1} as H-O-H bending vibration of adsorbed water. Table 1 details the weight composition of each vial containing a mixture of UiO-66 nanoparticles and liquid water and the respective FTIR O-H stretching analysis based on the length of the absorbance peaks and the area under the absorbance curve.

Table 1: Weight of UiO-66 and liquid water in vials and corresponding FTIR O-H stretching analysis

Vial#	Empty vial (mg)	UiO-66 + vial (mg)	UiO-66 + vial + water (mg)	Water (mg)	UiO-66 (mg)	Area of O-H stretching region	Peak % absorbance in O-H stretching region
1	1083.3	1087.3	1087.3	0	4	8293	11.11
2	1090.7	1092.7	1095.4	2.7	2	24173	39.62
3	1087.0	1102.5	1122.5	20	15.5	25157	40.17
4	1080.3	1089.0	1098.5	9.5	8.7	25519	41.50
5	1113.6	1117.1	1122.0	114.9	3.5	24819	42.10
6	1116.3	1117.5	1119.8	2.3	1.2	18450	32.11
7	1083.3	1084.5	1087.0	2.5	1.2	24481	41.43
8	1090.3	1090.9	1093.3	2.4	0.6	24271	43.29

Figure 1 shows the FTIR spectra of all eight (8) samples presented in Table 1. The spectral region encompassing wavenumbers 3700 cm^{-1} and 2852 cm^{-1} was selected and highlighted for quantifying water adsorption. The integrated absorbance within this band, i.e. the highlighted area under the absorbance curve, was calculated. Additionally, the peak absorbance at the characteristic O-H stretching wavenumber of 3352 cm^{-1} [12] was recorded as presented in Table 1. A strong linear correlation with a coefficient of determination R^2=0.9771 was observed between the integrated absorbance and peak absorbance, indicating that both parameters can be reliably employed as quantitative indicators of water adsorption. The bar graph in Figure 2 shows the weight percent of water and UiO-66 added to each vial. Red points show the percent absorbance values of FTIR spectra at 3352 cm^{-1} for the samples taken from the respective vials. The dry sample in vial 1 shows the lowest peak at the characteristic O-H stretching absorbance peak. All the remaining seven samples were wetted completely with water. This is clear in Figure 2 that the signature O-H stretching peak intensity at 3352 cm^{-1} increased considerably compared to the dry sample, which does not have a clear peak around 3352 cm^{-1}.

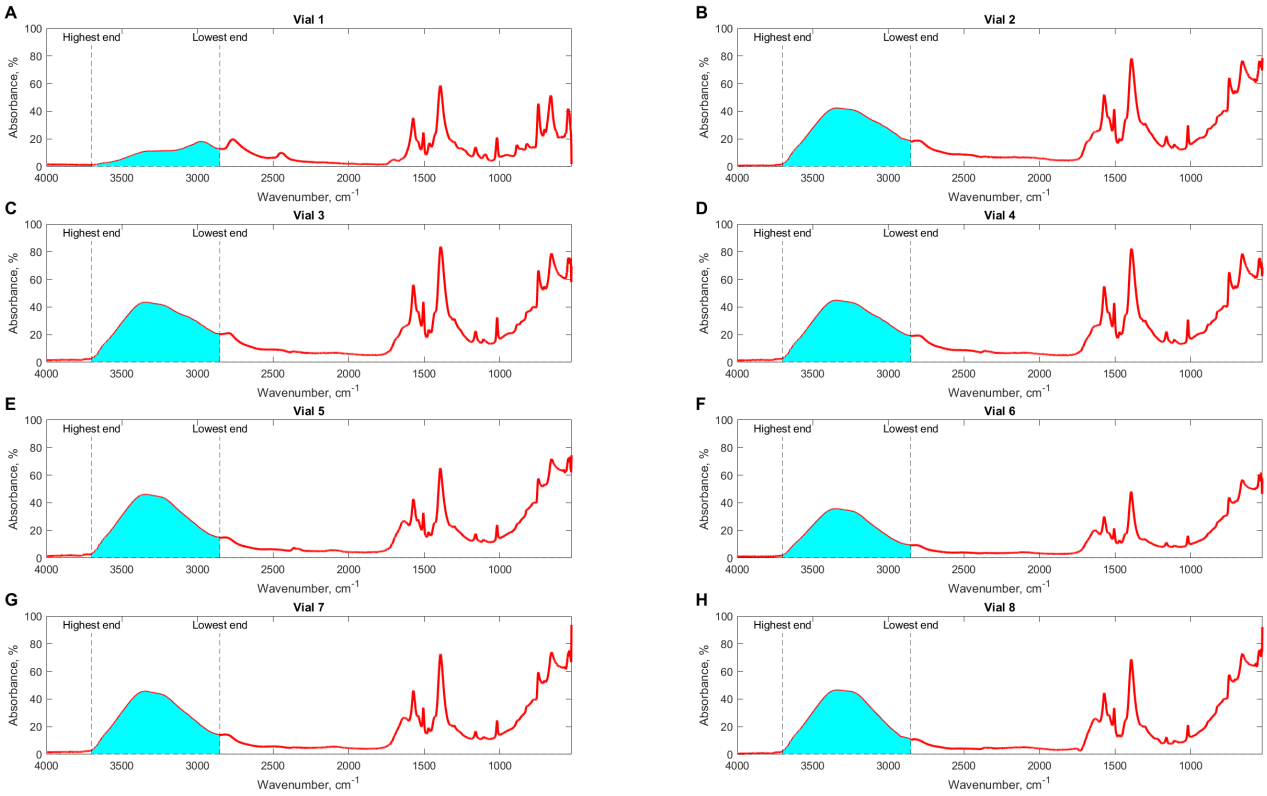

Fig. 1: FTIR absorbance spectra of UiO-66 nanoparticles in eight samples with O-H stretching regime between 3700-2852 cm^{-1} highlighted

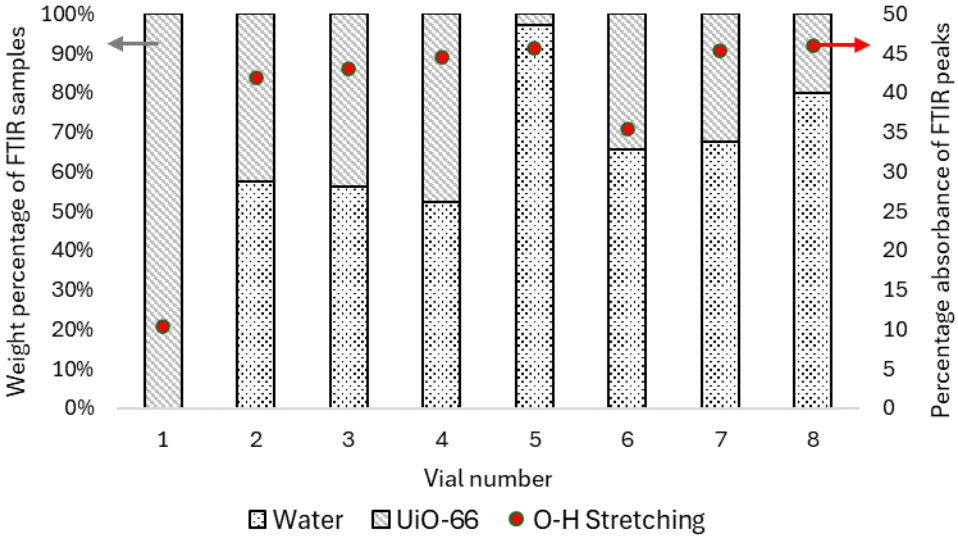

Fig. 2: Weight percent of water and UiO-66 nanoparticles in eight samples and the corresponding FTIR O-H stretching peak absorbance at 3352 cm^{-1}

Figures 1 and 2 show that amongst the seven wetted samples in vials 2-8, there is no visible trend between the O-H stretching peak and the amount of water added. Despite varying the added quantities, there was no significant change in the area under the peaks as the maximum adsorption capacity was reached. Considering that all eight samples comprised the same material, this outcome was anticipated. All seven samples, excluding the control, were wetted well enough to saturate the surface of the porous structure with water at the temperature of 30 °C and working pressure of 1 bar.

Adsorption of water molecules from water vapor was investigated at five different RH values. At low RH, the water adsorbed in time reaches a constant value faster than at higher RH values. The sample at an RH of 60% was kept overnight and an increase in the adsorbed water was observed. This data point collected at t = 53310 seconds is excluded from Figure 3A for improved clarity of the figure. In Figure 3B, the final equilibrium value for adsorbed water at each RH value is presented. Low water uptake at low RH values was reported as a characteristic of hydrophobic pore structures [14] and the initial filling of secondary building units (SBUs) [15]. The water uptake shown in Figure 3B is in agreement with the literature [16] except at the RH of 75%, which is observed considerably higher in this study. The trend shows an increase in water vapor adsorption at elevated RH values with a sharp jump at RH=75%, which might be related to interparticle condensation [15].

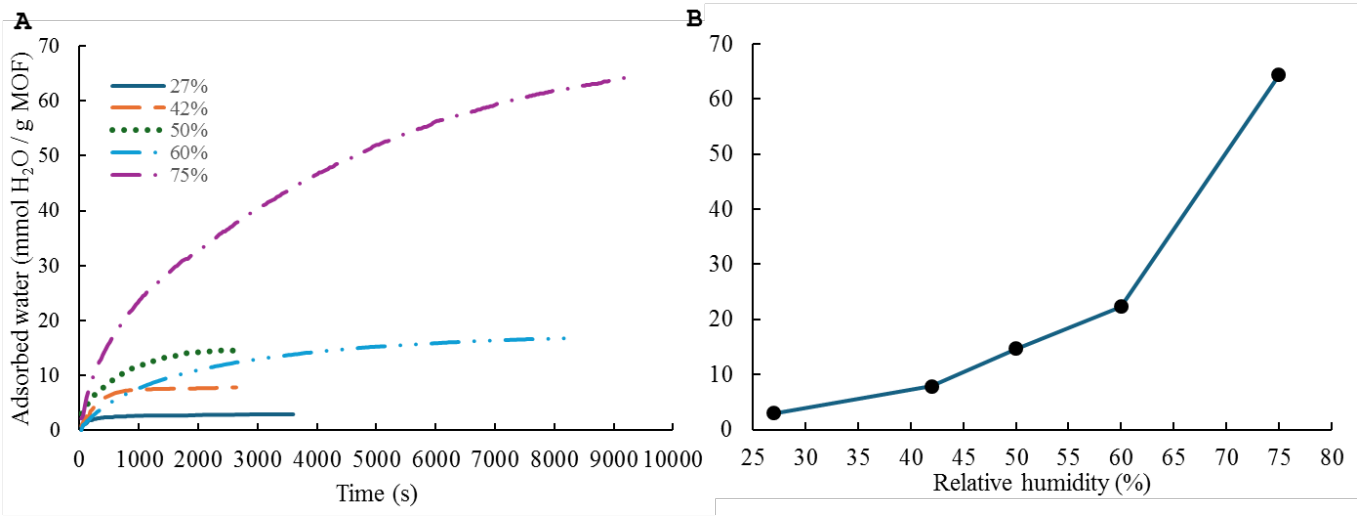

Fig. 3: Amount of water adsorbed in UiO-66 nanoparticles from humid air (A) at different RH values as a function of time and (B) the total equilibrium value reached at different RH values

4. Conclusion

In this study, adsorption of water molecules on zirconium based UiO-66 crystals from both liquid water phase and water vapor phase was conducted experimentally. Synthesized UiO-66 MOF nanoparticles were divided into samples for adsorption studies. Liquid water adsorption experiments show that it is possible to observe an increase at the characteristic O-H stretching peak in the FTIR spectra when the samples were wetted with water. Experiments for water vapor adsorption show that UiO-66 MOF nanoparticles have higher water adsorption capacity at increasing RH values. Further studies with the FTIR characterization of UiO-66 nanoparticles from water vapor adsorption or liquid water adsorption at various working pressures (p/p_0) might give more insight to the water adsorption performance of UiO-66 nanoparticles. These MOF structures are promising for future applications of direct water adsorption from ambient air. Studies improving the accessibility to drinking water become more important every day, therefore solutions to obtain clean water with low energy consumption play a key role in the MOF research.

Acknowledgements

Financial support for this research was provided by The Scientific and Technological Research Council of Turkiye (TUBITAK) through project number 220M002 and Hacettepe University BAP grant number FHD-2024-20812. Author Saziye Dere was supported by the TUBITAK 2247-C STAR Researcher Training Programme for high school teachers as part of project 220M002.

References

[1] B. L. Chen, M. Eddaoudi, S. T. Hyde, M. O'Keeffe, and O. M. Yaghi, "Interwoven metal-organic framework on a periodic minimal surface with extra-large pores," *Science,* vol. 291, no. 5506, pp. 1021-1023, Feb 2001, doi: 10.1126/science.1056598.

[2] M. Eddaoudi, H. L. Li, and O. M. Yaghi, "Highly porous and stable metal-organic frameworks: Structure design and sorption properties," *Journal of the American Chemical Society,* vol. 122, no. 7, pp. 1391-1397, Feb 2000, doi: 10.1021/ja9933386.

[3] L. Alaerts, C. E. A. Kirschhock, M. Maes, M. A. van der Veen, V. Finsy, A. Depla, J. A. Martens, G. V. Baron, P. A. Jacobs, J. F. M. Denayer, and D. E. De Vos, "Selective adsorption and separation of xylene isomers and ethylbenzene with the microporous vanadium(IV) terephthalate MIL-47," *Angew. Chem.-Int. Edit.,* vol. 46, no. 23, pp. 4293-4297, 2007, doi: 10.1002/anie.200700056.

[4] C. H. Hendon, D. Tiana, M. Fontecave, C. Sanchez, L. D'arras, C. Sassoye, L. Rozes, C. Mellot-Draznieks, and A. Walsh, "Engineering the Optical Response of the Titanium-MIL-125 Metal-Organic Framework through Ligand Functionalization," *Journal of the American Chemical Society,* vol. 135, no. 30, pp. 10942-10945, Jul 2013, doi: 10.1021/ja405350u.

[5] P. S. Bárcia, D. Guimarães, P. A. P. Mendes, J. A. C. Silva, V. Guillerm, H. Chevreau, C. Serre, A. E. Rodrigues, "Reverse shape selectivity in the adsorption of hexane and xylene isomers in MOF UiO-66," *Microporous Mesoporous Mat.,* vol. 139, no. 1-3, pp. 67-73, Mar 2011, doi: 10.1016/j.micromeso.2010.10.019.

[6] Q. Y. Yang, A. D. Wiersum, H. Jobic, V. Guillerm, C. Serre, P. L. Llewellyn, and G. Maurin, "Understanding the Thermodynamic and Kinetic Behavior of the CO_2/CH_4 Gas Mixture within the Porous Zirconium Terephthalate UiO-66(Zr): A Joint Experimental and Modeling Approach," *J. Phys. Chem. C,* vol. 115, no. 28, pp. 13768-13774, Jul 2011, doi: 10.1021/jp202633t.

[7] Q. Y. Yang, A. D. Wiersum, P. L. Llewellyn, V. Guillerm, C. Serred, and G. Maurin, "Functionalizing porous zirconium terephthalate UiO-66(Zr) for natural gas upgrading: a computational exploration," *Chem. Commun.,* vol. 47, no. 34, pp. 9603-9605, 2011, doi: 10.1039/c1cc13543k.

[8] T. Z. Wasti, M. Sultan, M. Aleem, U. Sajjad, M. Farooq, H. M. U. Raza, M. U. Khan, and S. Noor, "An overview of solid and liquid materials for adsorption-based atmospheric water harvesting," *Advances in Mechanical Engineering,* vol. 14, pp. 1-27, 03/02 2022, doi: 10.1177/16878132221082768.

[9] H. Furukawa, F. Gándara, Y.-B. Zhang, J. Jiang, W. L. Queen, M. R. Hudson, and O. M. Yaghi, "Water Adsorption in Porous Metal–Organic Frameworks and Related Materials," *Journal of the American Chemical Society,* vol. 136, no. 11, pp. 4369-4381, 2014/03/19 2014, doi: 10.1021/ja500330a.

[10] X.-M. Zhang M.-L. Li, W.-T. Yang, Q.-Y. Wang, S.-C. Liu, C.-W. Zhang, Y.-T. Cao, and G.-J. Wang, "A general strategy for MOFs coupled to optical fiber for highly sensitive humidity sensing," *Rare Metals,* vol. 42, no. 6, pp. 1821-1828, Jun 2023, doi: 10.1007/s12598-022-02245-1.

[11] F. Trapani, A. Polyzoidis, S. Loebbecke, and C. G. Piscopo, "On the general water harvesting capability of metal-organic frameworks under well-defined climatic conditions," (in English), *Microporous Mesoporous Mat.,* vol. 230, pp. 20-24, Aug 2016, doi: 10.1016/j.micromeso.2016.04.040.

[12] F.-F. Lu, X.-W. Gu, E. Wu, B. Li, and G. Qian, "Systematic evaluation of water adsorption in isoreticular UiO-type metal–organic frameworks," *Journal of Materials Chemistry A,* 10.1039/D2TA07392G vol. 11, no. 3, pp. 1246-1255, 2023, doi: 10.1039/D2TA07392G.

[13] X. Guo, L. Liu, J. Wu, J. Fan, and Y. Wu, "Qualitatively and quantitatively characterizing water adsorption of a cellulose nanofiber film using micro-FTIR spectroscopy," *RSC Advances,* 10.1039/C7RA09894D vol. 8, no. 8, pp. 4214-4220, 2018, doi: 10.1039/C7RA09894D.
[14] M. Steinert, S. J. Ernst, and S. Henninger, "Metal-Organic Frameworks as Sorption Materials for Heat Transformation Processes," *Eur J Inorg Chem,* vol. 2020, pp. 4502-4515, 11/19 2020, doi: 10.1002/ejic.202000834.
[15] F. Jeremias, V. Lozan, S. K. Henninger, and C. Janiak, "Programming MOFs for water sorption: amino-functionalized MIL-125 and UiO-66 for heat transformation and heat storage applications," *Dalton Transactions,* 10.1039/C3DT51471D vol. 42, no. 45, pp. 15967-15973, 2013, doi: 10.1039/C3DT51471D.
[16] G. E. Cmarik, M. Kim, S. M. Cohen, and K. S. Walton, "Tuning the Adsorption Properties of UiO-66 via Ligand Functionalization," *Langmuir,* vol. 28, no. 44, pp. 15606-15613, 2012/11/06 2012, doi: 10.1021/la3035352.